

Theory of uniaxial and biaxial nematic phases in bent-core systems

B. Mettout

LPTM, 33 rue St Leu, 80000 Amiens, France

(Received 27 August 2004; revised manuscript received 4 May 2005; published 16 September 2005)

We present a phenomenological theory of the uniaxial and biaxial nematic phases recently observed in bent-core mesogenic systems. To take into account the molecular anisotropy we introduce two types of symmetry transformation: “external” rotations which turn the molecules with respect to the laboratory axes and “internal” rotations which turn them with respect to the molecular axes. We show then that the description of bent-core nematic phases involves two isomorphic copies of the conventional tensor order parameter instead of one for conventional rod like and disk like molecules. The second tensor stabilizes additional monoclinic and triclinic phases and merges the calamitic and diskotic uniaxial states into a single phase. The uniaxial and biaxial phases can appear, respectively, in six and 21 distinct configurations according to the molecular axis that dominates the ordering process. We predict a number of isostructural transitions between these configurations within a thermodynamic Landau-type approach. Because bent-core molecules have the same microscopic behavior as orthorhombic micelles, the biaxial phase can be stabilized in both systems.

DOI: [10.1103/PhysRevE.72.031706](https://doi.org/10.1103/PhysRevE.72.031706)

PACS number(s): 64.70.Md, 61.30.Cz

I. INTRODUCTION

The macroscopic properties of mesophases composed of bent-core molecules [1] are reminiscent of their unusual shape and symmetry [2]. The polar character and the strong anisotropy of the orthorhombic molecular group facilitates the formation of low-symmetry antiferroelectric smectic phases while they prevent usually the cylindrically symmetric nematic and smectic-*A* phases. These latter structures are quite rare in pure bent-core systems and are only observed for the less bent molecules [3]. This feature is confirmed by numerical simulations [4]. Along the same way, smaller-angle nematic phases can only be obtained in mixtures with straight-core molecules [5]. On the other hand they display the first unambiguous evidence of biaxiality in thermotropic nematic phases [6]. Since the theoretical prediction of biaxial nematics by Freiser in 1970 [7] and their first observation in lyotropic mesophases, their existence in thermotropic liquid crystals has remained controversial.

In bent-core systems, the rarity of nematics on the one hand and their (relatively) easy biaxiality on the other hand is a paradoxical situation which demands a theoretical clarification. The simple argument stating that a nematic phase is preferentially biaxial in bent-core systems because the molecules are biaxial is obviously not sufficient. Indeed, all the molecules forming conventional uniaxial phases also actually have low-symmetry groups and nevertheless always form symmetric states. The distinction between conventional and unconventional systems is more subtle and needs a detailed analysis of the relations between macroscopic and molecular symmetries. Let us denote temporarily as “conventional” the uniaxial nematics formed with disklike or rodlike molecules, and “unconventional” the uniaxial and biaxial phases observed in bent-core systems. Along these lines a conventional molecule has a single distinguished direction parallel to the rod or normal to the disk (which can possibly coincide with a molecular symmetry axis) while a bent-core molecule has three perpendicular distinguished directions.

This distinction turns out to be crucial when one addresses the question: How are the molecules oriented in the

uniaxial phase? In conventional mesophases the principal molecular axis is oriented parallel to the macroscopic optic axis and the molecule spins around it. Such molecules can thus be characterized by their statistical tendency to form microscopic cylinders. In bent-core systems matters are not so simple because molecules without one single distinguished axis cannot exhibit this tendency. The answer to the previous question becomes in that case necessarily more intricate and must be found in a thorough statistical analysis of the unconventional phases. In the classical theory of nematics [8,9] the probability distribution of molecular orientation depends on a *single tensor order parameter*. It predicts, in the uniaxial phase, the same spinning process as we described above for disk like and rod like molecules. This approach is therefore very successful for conventional systems. However, in bent-core and lyotropic systems it fails for two reasons. (i) As we shall show below it applies only to a limited class of “uniaxial” molecules, excluding orthorhombic bent-core molecules and micelles. (ii) It is incomplete since it cannot foresee the lowest symmetric phases (with monoclinic C_{2h} and triclinic C_i point groups) that can be stabilized with second-rank tensors. The remedy is the same for both flaws: Taking as order parameters several second-rank tensors to describe the orientation ordering of unconventional molecules. This results from a natural generalization of the classical statistical description of rod like molecules when one attempts to describe the behavior of the molecular axes normal to the main axis. We have already used this multi tensor approach to overcome a similar incompleteness in the Landau theory of *s*-wave pairing superconductors [10] and to explain the low-symmetry polar nematic phases observed in copolyester compounds [11]. In nonpolar nematic phases, one can show that two second-rank tensors are sufficient to achieve the phenomenological approach and to define completely the orientation order of orthorhombic molecules. A complete description of the symmetry-breaking orientational ordering in bent-core nematics is then provided by the ten components associated with these two tensors (which are similar to the nine statistical functions proposed

by Straley [12] in a mean field theory for molecules lacking an axis of symmetry).

A multi tensor theory of bent-core nematics has already been proposed by Lubensky and Radzihovsky [13]. The order parameter assumed by these authors is formed by a combination of vectors and second- and third-rank tensors. Although it takes into account a single second-rank tensor, this theory yields a wide nematic polymorphism but it does not predict ordered phases with C_{2h} and C_i point groups. Moreover this polymorphism has not yet been evidenced.

We will show that the statistical behavior of one molecule depends essentially on its symmetry. More precisely, all the molecules with a group belonging to a definite class of symmetry groups exhibit the same qualitative properties in the nematic phases. In the first class of molecules, which corresponds to the “uniaxial molecular groups” $C_3, C_{3v}, C_4, D_4, \dots, D_{\infty h}$, the statistical description of the nematic phases depends on a single second-rank tensor. Strictly speaking we define as a conventional system any uniaxial or biaxial nematic phase made with such molecules. All the others are unconventional. The main property of conventional systems is that the molecular axes normal to the (three fold, fourfold etc.) symmetry axis of the molecule remain disordered. However, it is known that most of the nematogen molecules studied as yet are also well described by a single tensor, even when their symmetry is not in the conventional class. Indeed for asymmetric stick like and disklike molecules the ordering of the “small” axes plays a minor role in the properties of the ordered nematic phases, and can be considered at a first approximation as a negligible secondary effect. Then, roughly speaking, we will denote these systems also as conventional. In other words, the conventional description (one tensor) may apply exactly to uniaxial molecules and approximately to asymmetric stick like and disklike molecules. Reciprocally, an unconventional system is one with nonuniaxial molecules which cannot be described, even approximately, by a single tensor, i.e., in which the ordering of all the molecular axes plays a non-negligible role.

The bent-core molecules belong to an unconventional class that contains only the orthorhombic groups C_{2v}, D_2 , and D_{2h} . The corresponding molecules exhibit similar statistical behaviors in the nematic phases. It is interesting to notice that the only biaxial phases known before the discovery of bent-core molecules were observed in lyotropic systems in which the molecules form micelles with D_{2h} symmetry surrounded by water, i.e., belonging to the same class as bent-core molecules. This coincidence between the statistical descriptions of both systems permits us to extend the approach presented in this paper to micelles with only minor modifications. Indeed, many facts reported in the following sections are described in terms of a fluctuating “subunit” with D_{2h} symmetry which can represent a virtual average bent-core molecule as well as a micelle. We will discuss in the last section the relevance of our approach to lyotropics and the main differences between the two systems.

II. STATISTICAL DESCRIPTION OF UNCONVENTIONAL NEMATIC PHASES

The conventional description of nematic phases [8,9] involves a single order parameter which transforms as a

second-rank tensor under the symmetry operations of the rotation group. Its five components η_m ($-2 \leq m \leq 2$) describe the orientation in space of the main axis of stick like or disklike molecules. In such systems the molecules are characterized by the presence of a distinguished direction (parallel to the stick or normal to the disk). In the uniaxial nematic phase the probability to find the molecular axis in the direction given by the spherical angles θ, φ is, in the first-harmonic approximation, given by

$$P(\theta, \varphi) \approx P_0 + \eta_0 \frac{3 \cos^2 \theta - 1}{2}. \quad (1)$$

The omitted higher harmonics (i.e., transforming as tensors with rank > 2) either cancel or are non-symmetry-breaking “secondary order parameters” which cannot change qualitatively the properties of the stable phases. When the order parameter η_0 is positive the maximum of the distribution corresponds to an alignment of the molecular axis along the macroscopic optic axis Oz (calamitic phase) whereas when $\eta_0 < 0$ the molecular axis is preferentially oriented in the plane perpendicular to the optic axis (diskotic phase) and its direction is disordered within this plane. This latter configuration is quite unlikely for steric reasons for stick like as well as disklike molecules. It should not be confused with the actual nematic configuration of disklike molecules which corresponds to the calamitic distribution [i.e., with $\eta_0 > 0$ in Eq. (1)] of the molecular axis normal to the disk.

In the domain of the biaxial nematic phase [7] in which the principal axes of the tensor are aligned along Ox, Oy , and Oz , an additional asymmetric term appears in P :

$$P(\theta, \varphi) = P_0 + \eta_0 \frac{3 \cos^2 \theta - 1}{2} + \eta_2 \frac{\sqrt{3}}{2} \sin^2 \theta \cos 2\varphi. \quad (2)$$

When $\eta_2 = 0$ or $\pm \sqrt{3} \eta_0$ the phase is uniaxial (see Fig. 1) with the molecular axis preferentially oriented along Oz, Oy , or Ox , respectively. A three fold rotation in the η_0, η_2 order-parameter space is equivalent to a circular permutation of the axes x, y, z whereas the transformation $\eta_2 \leftrightarrow -\eta_2$ permutes x and y . The sectors denoted $B2$ to $B6$ correspond to the five other domains obtained from $B1$ after permuting x, y, z .

When $\eta_2 = 0$ and $\eta_0 > 0$, the phase is uniaxial calamitic and the maximum of the distribution arises when the molecular axis is parallel to Oz [$C(z)$ in Fig. 1]. The fluctuations around the maximum are symmetric, i.e., the probability for the axis to tilt is independent of the direction of the tilting plane. When η_2 becomes positive the molecules remain preferentially oriented along Oz as in the uniaxial phase. However, the distribution of the molecules fluctuating around the maximum is anisotropic so that it is more likely to find one molecule tilted in the plane Oxz ($B1$ in Fig. 1). When η_2 increases, the fluctuation amplitude increases until $\eta_2 = \sqrt{3} \eta_0$ where the probability of orientation becomes identical in all the directions of the Oxz plane [giving rise to the uniaxial diskotic phase denoted $D(xz)$ in Fig. 1].

An important thermodynamic feature of this model emerges in Fig. 1. The calamitic and diskotic structures are distinct phases though they exhibit the same symmetry group. Indeed, there exist only two ways in the order-

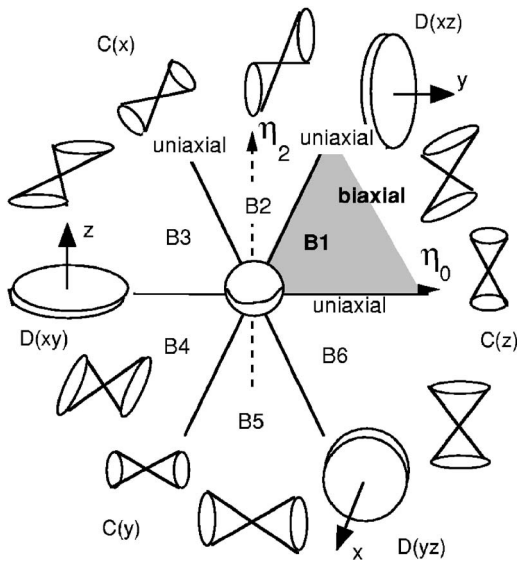


FIG. 1. Schematic representation of the distribution function P [Eq. (2)] in the order-parameter space of the conventional biaxial phase. The main fluctuations of the stick like molecules are schematized by a cone. For $\eta_2 = \eta_0 = 0$ the phase is isotropic and the cone is a sphere (same probability in all directions). In the uniaxial calamitic phase [$C(x)$, $C(y)$, and $C(z)$] the molecule is preferentially oriented along one direction (x , y or z) and fluctuates isotropically around it (symmetric cone). In the biaxial phase (B1 to B6) the fluctuations around the preferred axis are anisotropic and lead to a flat cone. The anisotropy and the amplitude of the fluctuations increase when going from calamitic to diskotic. In the uniaxial diskotic phase [$D(xy)$, $D(xz)$ and $D(yz)$] the molecular orientation is completely disordered in one plane [e.g., Oxy for $D(xy)$] and the cone becomes a disk. For instance in the sector B1 the preferred direction is Oz and the fluctuations are in the Oxz plane whereas in B6 the fluctuations are in Oyz . All the nonequivalent states lie within the gray sector B1. The other sectors correspond to domains of the same states: B3 and B5 are obtained from B1 by $2\pi/3$ and $4\pi/3$ external rotations around the direction (111) whereas B6, B4, and B2 are obtained from B1, B3, and B5, respectively, after four-fold rotations around Oz .

parameter space for transforming continuously the diskotic configuration into the calamitic one: either by crossing the isotropic phase at $\eta_2 = \eta_0 = 0$ or by going through the biaxial phase in sector B1. In the two cases the transformation is accompanied by two phase transitions. The impossibility of going continuously from the diskotic to the calamitic configuration without any phase transition is the signature of distinct phases. A first-order phase transition can, of course, also happen between the two phases. However, despite the identity of their symmetry groups, this transition is not of the liquid-gas type (isostructural), i.e., the corresponding transition line has no end critical point beyond which the two phases could transform continuously one into the other. This is characteristic of an *anti-isostructural transition* [14]. Such a transition permits in particular the existence of a Landau four-phase point [12] in the phase diagram where the isotropic liquid, and the biaxial and two uniaxial phases can coexist.

One can show (see the Appendix) that the previous one-tensor model is exact for molecular symmetries containing at

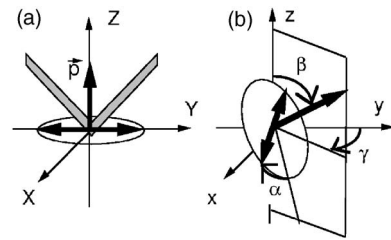


FIG. 2. (a) The three main axes X, Y, Z of one bent-core molecule. The molecular polarization p lies along the two fold symmetry axis Z . (b) Euler angles α, β, γ characterizing the orientation of one molecule in the laboratory frame Ox, y, z .

least one distinguished rotation axis (which we will call “uniaxial molecules” in the following) of order higher than 2 ($C_3, C_{3v}, D_4, \dots, D_{\infty h}$). In the uniaxial as well as in the biaxial phases, all the molecules in this series rotate about their special axis to form cylindrically symmetric subunits. For less symmetric molecules this model neglects the corrections due to the actual molecular anisotropy. In the case of asymmetric stick like and disklike molecules these corrections are small, and the model provides a fair approximation of the real behavior. In the case of strongly anisotropic objects, as for instance the biaxial bent-core molecules or matchboxlike micelles in lyotropic fluids, the corrections are not small and a more complete description is needed. In the general case of molecules with no symmetry, five second-rank tensors are necessary for a complete description. This number decreases with increasing molecular symmetry, down to 1 for uniaxial molecules or even to zero for optically isotropic molecules [with molecular symmetry groups $O(3), O, O_h, T, T_d$, etc.].

Let us denote by α, β, γ the three Euler angles that characterize the orientation of a given molecule with respect to the laboratory frame (Fig. 2). In the nematic phases the orientation distribution $P(\alpha, \beta, \gamma)$ which generalizes Eq. (1) can be written (see, for instance, [15])

$$P(\alpha, \beta, \gamma) = P_0 + \sum_{m=-2}^2 \sum_{p=-2}^2 \eta_{m,p} D_{m,p}^2(\alpha, \beta, \gamma) \quad (3)$$

where P_0 is a normalization constant and $D_{m,p}^2$ are Euler spherical functions [16]. The coefficients $\eta_{m,p}$ constitute the 25 components of the full order parameter. $D_{m,p}^2$ transforms as Y_m^2 under (external) rotations with respect to the laboratory frame and as Y_p^2 under (internal) rotations with respect to the molecular frames. The difference between these two types of symmetry transformations is the key idea of our analysis.

The difference between usual (external) and molecular (internal) rotations is illustrated in Fig. 3. Both act on the distribution P , but in different ways. This distribution may be visualized as a set of molecules, each one with a given orientation and a given statistical weight. An external rotation (say C_{2y}) turns all the molecules in the set by an angle π with respect to the fixed axis Oy of the laboratory frame, in such a way that the relative orientation of two molecules in the set is preserved [Fig. 3(b)]. Contrariwise, an internal rotation turns each molecule by an angle π with respect to the axis

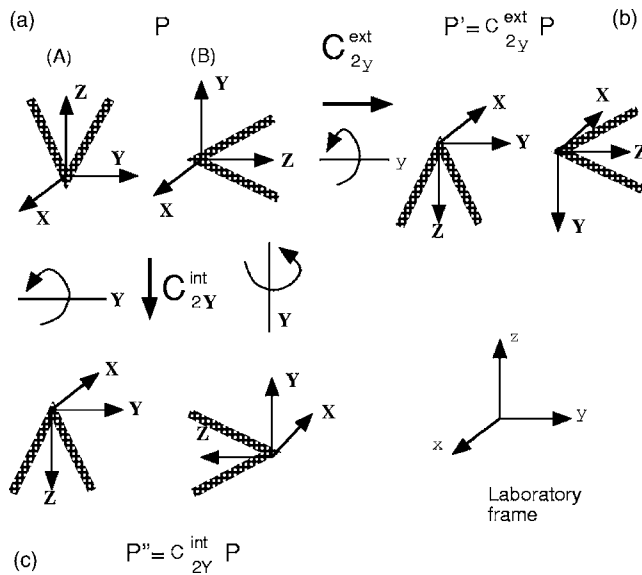


FIG. 3. Action of external and internal symmetries upon the statistical distribution P . (a) P is represented by a set of molecules oriented in various directions. Two of them are represented in the figure. The figure can also be understood as a distribution containing only two possible orientations (A and B) with probabilities $1/2$. x, y, z are the fixed axes of the laboratory frame and X, Y, Z represent the frames rigidly tied to the molecules. (b) Under an external two fold rotation around Oy the orientation A is reversed whereas B is unchanged. The new distribution P' gives probabilities $1/2$ for the two new orientations and is equivalent to P seen by an observer rotated in the laboratory frame. (c) Under an internal two fold rotation around OY the configuration A rotates around Oy and is still reversed whereas the configuration B is rotated around Oz and is also reversed. The corresponding distribution P'' is different from P' . This example illustrates the difference between C_{2y}^{int} and C_{2y}^{ext} . P'' is not equivalent to P seen by any rotated observer.

OY of that molecule before the rotation. Since the initial orientations of two molecules in the set are different, they are actually rotated with respect to two different laboratory axes [Fig. 3(c)]. The relative orientation of the molecules in the set is thus modified by the internal operation. Consequently, although the free energy $F(P)$ is invariant under external symmetries, it is in general modified by internal transformations. Thermodynamic properties are thus essentially constrained by external operations. Internal symmetries provide classificatory rules which determine the description of one given phase (e.g., number of independent degrees of freedom) for various types of molecules.

The distinction between internal and external transformations permits us to classify the distributions (3) according to the usual rotation group $O^{ext}(3)$ on the one hand, and independently according to the molecular rotation group $O^{int}(3)$ on the other hand. One given distribution P is invariant with respect to an external group characteristic of the phase associated with the distribution: $O^{ext}(3)$ in the isotropic phase, $D_{\infty h}^{ext}$ in the uniaxial phase, D_{2h}^{ext} in the biaxial phase, and so on. The same distribution P is, of course, invariant under internal operations belonging to the actual symmetry group of the molecules, e.g., C_{2v} in bent-core systems (D_{2h} for micelles). Let us stress that, in addition to these evident internal sym-

metries, $P(\alpha, \beta, \gamma)$ can also be invariant under some internal operations which are out of the actual molecular group C_{2v} . These operations form the “effective molecular group” which contains C_{2v} as a proper subgroup. The molecules behave, at time scales larger than the mean molecular fluctuation time, exactly as effective subunits exhibiting the symmetries of the effective molecular group. This striking property is not surprising if one considers, for instance, the isotropic phase. Indeed, the distribution is in this case reduced to the constant term P_0 in Eq. (3) which is of course invariant under any external as well as any internal operation. Hence the effective molecular symmetry is $O^{int}(3)$ which is much larger than the discrete actual molecular group (except for a liquid consisting of isotropic atoms or micelles in which they coincide).

In order to understand the difference between internal and external operations and between the actual and the effective molecular group, let us first consider the nematic phases of a conventional system consisting of uniaxial molecules with C_{3v} symmetry. In order to make P invariant under this (internal) group it is necessary to cancel most of the order-parameter components in Eq. (3). The surviving $\eta_{m,p}$ correspond to $p=0$. Similarly, in the biaxial phase the external group D_{2h} cancels the $\eta_{m,0}$ with $m=\pm 1$ and imposes $\eta_{2,0} = \eta_{-2,0}$. The distribution $P(\alpha, \beta, \gamma)$ is then given by Eqs. (1) and (2) where θ and φ are the spherical coordinates of the three fold molecular axis C_3 ($\theta=\beta, \varphi=\gamma$) and where $\eta_0 = \eta_{0,0}$ and $\eta_2 = \eta_{2,0}$. It describes fluctuations in which the axes normal to C_3 are completely disordered. The corresponding sub-unit is a cylindrically symmetric object resulting from the dynamical rotation of the molecule around its distinguished axis. In the uniaxial phase [Eq. (1)] the effective molecular group $D_{\infty h}^{int}$ coincides with the external group $D_{\infty h}^{ext}$. On the contrary, in the biaxial phase [Eq. (2)] the effective molecular group $D_{\infty h}^{int}$ is more symmetric than the external group D_{2h}^{ext} . In both phases the subunit is a cylinder.

The subunit is defined as a composite statistical object that has the effective molecular symmetry, e.g., D_{2h} for bent-core molecules. It is built by superposing various molecules obtained from a single one on applying the operations of the effective group, each one with the same statistical weight. In the bent-core case two (=order of D_{2h}/C_{2v}) crossed molecules are superimposed with their XY planes parallel and their Z axes reversed (or a more complex superposition in the special states where the effective symmetry is raised to $D_{\infty h}^{int}$). The subunit permits one to describe in a simpler way the actual distribution function. Indeed, P has exactly the same mathematical form for all the objects belonging to the same class, in particular those with symmetry D_{2h} (maximal symmetry in the class). Then it is more convenient to describe P in terms of subunits than in terms of bent-core molecules. Stating that P contains N subunits with orientations $A_1, A_2, A_3, \dots, A_N$ means then that it contains in fact $2N$ bent-core molecules oriented as $A_{1+}, A_{1-}, A_{2+}, A_{2-}, \dots$ where A_{1+} and A_{1-} differ only by the sense of the molecular polarization Z . For instance stating that all the subunits are oriented with their axes X, Y, Z along x, y, z means that half of the bent-core molecules are oriented with X, Y, Z parallel to $x, y, +z$ and the other half with X, Y, Z oriented parallel to $x, y, -z$.

When the system is experimentally probed at frequencies lower than the mean molecular fluctuation time, it cannot be distinguished from a system consisting of molecules with symmetry D_{2h} .

Let us illustrate internal vs external symmetries with the following example. A distribution P invariant under internal rotations around Z (cylindrical subunit) is different from a distribution invariant under the external rotations around z (macroscopically uniaxial). In the former, when one orientation of the molecule is permitted then all the orientations turned around Z are also permitted with the same statistical weight. In the latter, when one orientation is permitted then all the orientations turned around z are also permitted with the same weight. These two criteria are completely independent. For instance, a distribution can be cylindrically symmetric with respect to internal operations and macroscopically biaxial when the distribution of the resulting cylinder axis is given by Eq. (2). Reciprocally a distribution of bent-core molecules can be cylindrically symmetric at the macroscopic level and microscopically biaxial (D_{2h}) [this is the case for instance when the distribution is given by Eq. (5) of Sec. III, which describes the orientation of bent-core molecules in the unconventional uniaxial phase where the three molecular axes participate to the ordering process].

Even for nonuniaxial molecules the actual molecular symmetries can be incompatible with several functions $D_{m,p}^2$ which, consequently, cannot appear in expansion (3). The corresponding forbidden $\eta_{m,p}$ vanish identically. For bent-core molecules with C_{2v} symmetry group, only ten components are permitted, for $p=0$ and ± 2 , so that the distribution reads

$$P(\alpha, \beta, \gamma) = P_0 + \sum_{m=-2}^2 \eta_{m,0} D_{m,0}^2 + \eta'_{m,2} (D_{m,2}^2 + D_{m,-2}^2) \quad (4)$$

where α, β, γ are defined in Fig. 2(b). In contrast with the one-tensor model, in this case the order parameter contains ten components, which split into two independent tensors $\eta = \{\eta_{m,0}\}$ and $\eta' = \{\eta'_{m,2}\}$. Since these two sets transform as the same irreducible representation of the isotropic (external) liquid group $O(3)$, they are denoted “pseudoproper” order parameters and they are bilinearly coupled in the free energy. Indeed, in any system there exists always one bilinear term coupling two order parameters transforming as the same representation of the high-symmetry phase [consider, for instance, two three-dimensional (3D) vectors r and r' ; their scalar product $r \cdot r'$ is a bilinear invariant of $O(3)$]. The most important consequence of the bilinear coupling is that there cannot exist separate phases defined by $\eta=0$ and $\eta' \neq 0$ (or conversely). The onset of one order parameter yields automatically the onset of the second one. For example, in the uniaxial nematic phase both η and η' take finite values. When continuous symmetries are broken (e.g., at the isotropic \leftrightarrow nematic transition), the presence of a second pseudoproper order parameter modifies the physical properties of the condensed phases in various respects (see, for instance, Refs. [10,11]).

(1) In addition to the conventional uniaxial and biaxial nematics, two ordered phases can be stabilized with ortho-

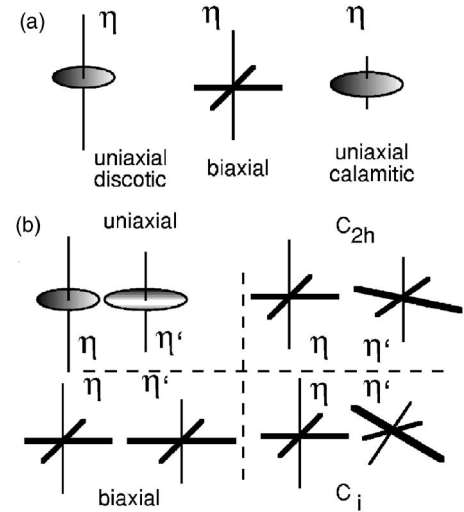


FIG. 4. Schematic representation of the equilibrium phases. (a) Conventional nematics. The single tensor order parameter η is represented in the biaxial state by its three proper directions. In the uniaxial states two directions become equivalent and the tensor is invariant under rotation around the third direction. The plane containing the two degenerate directions is represented by a disk. (b) Bent-core nematics described by two tensors η and η' . The external symmetry groups of the corresponding phase are given by the intersection of the two tensor groups. When η and η' are uniaxial and their axes are parallel, the phase is uniaxial since the continuous rotation axes of the two tensors coincide. When the two tensors are parallel and at least one of them is biaxial, the phase is biaxial. When they share only one common axis the symmetry is C_{2h} and it is C_i when they have not any common axis.

rhombic C_{2h} and monoclinic C_i point groups [17]. They are schematically represented in Fig. 4. Let us notice that in the two new phases the molecular symmetry C_{2v} is not a subgroup of the macroscopic point group, and reciprocally.

(2) Even in the uniaxial phase the subunit is not cylindrically symmetric (the effective molecular group is D_{2h}^{int} instead of $D_{\infty h}^{\text{int}}$), in contrast, for instance, to the conventional case of uniaxial molecules which, in this phase, spin isotropically around their principal axis. The reason is that for biaxial molecules the system cannot choose a single preferred molecular spinning axis. The fact that the effective symmetry is D_{2h}^{int} , which is rigorously demonstrated in the Appendix, results from the following simple argument. Consider an order parameter consisting of a single copy of the tensor (e.g., $\eta_{m,0}$ occurring for uniaxial molecules). It is well known that when a single component ($\eta_{0,0}$) is nonzero, the external symmetry is $D_{\infty h}^{\text{ext}}$ (uniaxial phase) whereas when two components are nonzero ($\eta_{0,0}$ and $\eta_{2,0} + \eta_{-2,0}$) the external symmetry is D_{2h}^{ext} (biaxial phase). Moreover, let us recall that internal symmetries act over the index p in $\eta_{m,p}$ precisely as external symmetries act over m . By analogy one sees that, in the uniaxial phase, when one copy of the tensor ($\eta_{0,0}$) is nonzero (uniaxial molecules), the internal symmetry is $D_{\infty h}^{\text{int}}$ while when two copies ($\eta_{0,0}$ and $\eta_{0,2} + \eta_{0,-2}$) are nonzero (bent-core molecules) the internal symmetry is D_{2h}^{int} .

(3) The *qualitative* difference between calamitic and discotic uniaxial phases disappears. By varying temperature or

concentration, the system can continuously change from the calamitic to the diskotic configuration without undergoing any phase transformation. It suffices to change the signs of η and η' at different temperatures (see the more refined discussion below). Then, at variance with conventional nematics, even when one order parameter vanishes, the system remains in the ordered phase since the second order parameter remains finite. Technically speaking, the transition is anti-isostructural [14] in conventional nematics and isostructural (i.e., of the liquid-gas type) for bent-core molecules or micellar systems. An immediate consequence of this fact is the instability of the four-phase point predicted by the conventional theory of nematics [7].

(4) A variety of *quantitatively* different uniaxial structures is permitted.

III. THE UNCONVENTIONAL UNIAXIAL PHASE

On choosing the macroscopic optic axis along Oz , the only non vanishing terms in Eq. (4) are η_0 and η'_0 . The probability distribution takes then the simplified form

$$P(\alpha, \beta, \gamma) = P_0 + \eta_0 \frac{3 \cos^2 \beta - 1}{2} + \eta'_0 \frac{\sqrt{3}}{2} \sin^2 \beta \cos 2\alpha \quad (5)$$

where $\eta_0 = \eta_{0,0}$ and $\eta'_0 = \sqrt{2} \eta_{0,2} = \sqrt{2} \eta_{0,-2}$. The unconventional feature of $P(\alpha, \beta, \gamma)$ in Eq. (5) with respect to Eq. (1) comes from the fact that it depends on a second angle α (in addition to $\beta = \theta$) which produces an ordering of the axes X, Y normal to the molecular two fold axis Z [Fig. 2(a)]. Let us stress that this ordering at the molecular level does not break the macroscopic continuous symmetry ($D_{\infty h}^{\text{ext}}$) of the uniaxial phase [in contrast with Eq. (2) in which the angle $\varphi = \gamma$ replaces α in Eq. (5)]. When $\eta'_0 = 0$, the conventional distribution (1) is restored and the effective molecular group is raised to $D_{\infty h}^{\text{int}}$ because the molecules rotate isotropically around Z . However the macroscopic symmetry of the phase is not changed when, by chance, $\eta'_0 = 0$ so that this condition does not define a new phase (a phase is defined by its symmetry with respect to the laboratory frame and not by its internal molecular group which does not constrain the free energy). In the general case ($\eta'_0 \neq 0$) the molecular rotation is no longer isotropic so that the effective molecular symmetry is only D_{2h}^{int} .

Equation (5) describes the distribution of the three molecular axes X, Y, Z simultaneously. It proves convenient to study the behavior of each axis separately by averaging $P(\alpha, \beta, \gamma)$ over the two other axes (e.g., for Z by integrating P over α). If one denotes $\theta_i, \varphi_i (i=X, Y, Z)$ the spherical coordinates of the three molecular axes, one finds the following "partial distributions:"

$$P_Z(\theta_Z, \phi_Z) = P_0 + \eta_0 \frac{3 \cos^2 \theta_Z - 1}{2},$$

$$P_Y(\theta_Y, \phi_Y) = P_0 + \left(-\frac{1}{2} \eta_0 - \frac{\sqrt{3}}{2} \eta'_0 \right) \frac{3 \cos^2 \theta_Y - 1}{2},$$

$$P_X(\theta_X, \phi_X) = P_0 + \left(-\frac{1}{2} \eta_0 + \frac{\sqrt{3}}{2} \eta'_0 \right) \frac{3 \cos^2 \theta_X - 1}{2}. \quad (6)$$

$P_Z(\theta_Z, \varphi_Z)$ gives the probability to find Z along the direction θ_Z, φ_Z in the laboratory frame, i.e., the number of molecules with Z oriented along θ_Z, φ_Z divided by the total number N of molecules. This number is obtained by summing the numbers of molecules $NP(\alpha, \beta = \theta_Z, \gamma = \varphi_Z)$ with Z oriented along θ_Z, φ_Z and X, Y oriented along α over all the possible values of α . The equivalent procedure for obtaining P_Y and P_X is given in the Appendix. Each P_i in Eq. (6) carries a limited part of the information contained in the complete distribution $P(\alpha, \beta, \gamma)$ given in Eq. (5). They all describe the behavior of one molecular axis associated with the same distribution P . P_X, P_Y , and P_Z have the conventional uniaxial form [Eq. (1)], but with distinct amplitudes which characterize the degree of ordering associated with each molecular axis.

Equations (6) provide a convenient way for visualizing important features of the molecular distribution. Indeed, the three corresponding partial amplitudes $\eta_0, -(1/2)\eta_0 - (\sqrt{3}/2)\eta'_0$, and $-(1/2)\eta_0 + (\sqrt{3}/2)\eta'_0$ are the projections of three vectors, one for each molecular axis, onto the horizontal line η_0 in the plane of the coefficients η_0, η'_0 [Fig. 5(a)]. These vectors form a symmetric three-branch star which accounts for the degree of ordering (size of the star) together with the type of ordering (orientation of the star) associated with $P(\alpha, \beta, \gamma)$. Each axis can be either in the calamitic (positive projection) or in the diskotic (negative projection) state. The figure shows that if two partial distributions are in the same state, then the third one must be in the opposite state. This property is evident in the simple case of elongated molecules for which the long molecular axis Z is oriented along the optic axis Oz [calamitic(C) distribution] while the two other molecular axes X and Y rotate isotropically in the plane Oxy [both being thus in the diskotic(D) configurations]. For bent-core molecules this can be achieved by a rotation around one of the molecular axes (e.g., Z) as shown in Fig. 5(c) (DDC configuration). The converse case when X and Y are calamitic and Z is diskotic is slightly more intricate. The rotation must happen around the intermediate molecular direction $X+Y$ as shown in Fig. 5(c) (CCD). The molecular polarization is distributed isotropically in the plane Oxy whereas the axes X and Y are parallel, on average, to the optic axis Oz .

In the general case the three axes play similar roles and six different configurations can be foreseen according to the diskotic or calamitic character of the partial distributions: $(P_X, P_Y, P_Z) = (\text{CDD}), (\text{DCC}), (\text{DCD}), (\text{CDC}), (\text{DDC}),$ or (CCD) . As stated above these configurations do not correspond to different phases since a transformation between them can happen after rotating the star in Fig. 5(a). During the rotation, the star size remains finite and neither the isotropic nor the biaxial intermediate phases take place in the process.

Figure 5(b) presents the regions corresponding to the six configurations in the order-parameter space. It is worthwhile to compare this diagram with that in Fig. 1 [together with Eqs. (2) and (5)]. In the latter diagram all the points corre-

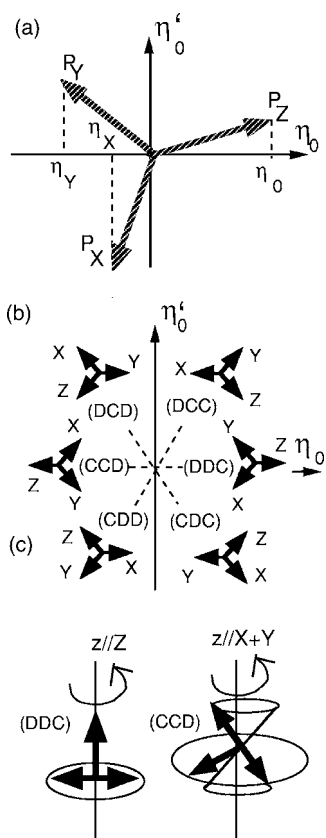


FIG. 5. (a) Three-branch star associated with the distribution $P(\alpha, \beta, \gamma)$ [Eq. (5)]. Each branch describes the fluctuations of X , Y , or Z . The projections $\eta_z = \eta_0$, $\eta_y = -(1/2)\eta_0 - (\sqrt{3}/2)\eta'_0$ and $\eta_x = -(1/2)\eta_0 + (\sqrt{3}/2)\eta'_0$ of each branch onto the horizontal axis coincide with the amplitudes of the partial orientation distributions of the corresponding axes [Eq. (6)]. (b) Positions, in the order-parameter space (η_0, η'_0) , of the six uniaxial configurations. On the middle of each region (indicated by dashed lines) a special state, occurring when one branch of the star becomes horizontal, is stabilized.

spond to distributions with cylindrical internal symmetry whereas the external symmetry is biaxial at general points and uniaxial on three specific lines. In the former diagram, which is the internal analog of the preceding, all the points have cylindrical external symmetries whereas the internal symmetry is biaxial at general points and uniaxial on specific lines. In Fig. 1, a three fold rotation corresponds to a permutation of the laboratory axes x, y, z [external rotation C_3 around the direction (111)] which transforms one domain into an equivalent domain with the same energy. In Fig. 5, a three fold rotation corresponds to a permutation of the molecular axes X, Y, Z [internal rotation C_3 around (111)].

The transformation between two configurations in Fig. 5 occurs when one vector in the star becomes vertical. Likewise, when one vector becomes horizontal a “special state,” with cylindrical effective molecular symmetry (characterized by the isotropic rotation of the molecules around the corresponding axis), is stabilized. Their positions in the order-parameter space are presented in Fig. 5(b).

State (i). $\eta'_0 = 0, P_z$ is horizontal. P coincides with P_z and with the conventional nematic distribution (1). The internal

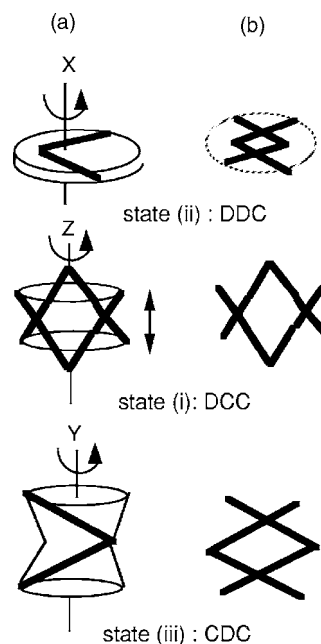


FIG. 6. (a) subunit shapes in the uniaxial special states. The subunits are generated by isotropic spinning of one bent-shape molecule (thick lines) around X, Y , or Z and, in state (ii), by up-down jumps between the two cones. (b) Corresponding subunits in the general states obtained by completely freezing the statistical internal spinning of molecules presented in (a). The three subunits have then the same form and the same orthorhombic symmetry.

fluctuations which give the subunit a cylindrical symmetry consist of an isotropic rotation around Z together with an “up-down” reversal process of the axis Z . They yield a double-cone-like subunit depicted in Fig. 6(a).

State (ii). $\eta_0 = \sqrt{3}\eta_0, P_x$ is horizontal. The molecules spin around X and the subunit takes the form of a flat disk. If one expresses the distribution P vs the Euler angles α', β', γ' defined as in Fig. 2 by replacing Z by X , then it coincides with the conventional nematic distribution (1) and with P_x .

State (iii). $\eta'_0 = \sqrt{3}\eta_0, P_y$ is horizontal. The molecules spin around Y and the subunit takes the cylindrical form described in Fig. 6(a). If one expresses the distribution P vs the Euler angles $\alpha'', \beta'', \gamma''$ defined as in Fig. 2 by replacing Z by Y then it coincides with the conventional nematic distribution (1) and with P_y .

In the three cases the subunit is cylindrically symmetric and nonpolar. $P(\alpha, \beta, \gamma)$ represents then the conventional nematic distribution for the single subunit axis and appears in two non equivalent (globally) calamitic (e.g., CDD) and diskotic (e.g., DCC) special states. The calamitic state is easy to visualize as a superposition of fixed subunits with almost parallel axes. In the diskotic state the subunit axis is disordered, with equal probability to be found in any direction normal to the macroscopic optic axis.

In the general case ($\eta_0 \neq 0, \eta'_0 \neq \pm\sqrt{3}\eta_0$) the distribution loses the accidental continuous degeneracy of the special states. Thus the molecular spinning is frozen and the effective symmetry group (D_{2h}^{int}) remains non polar but becomes discrete (recall that the macroscopic symmetry of the uniaxial nematic phase is $D_{\infty h}^{ext}$ and should not be confused

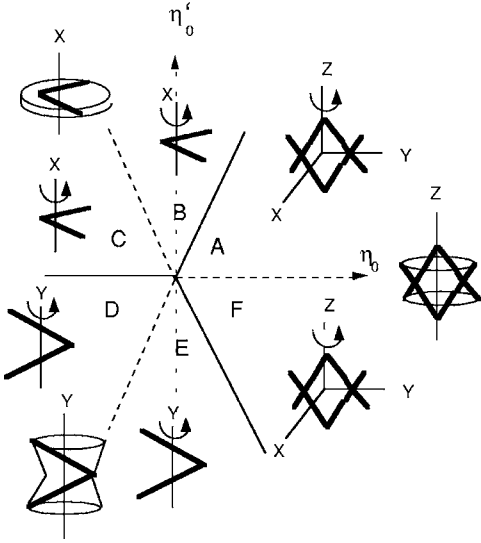


FIG. 7. Most likely orientations of the subunit in the unconventional uniaxial states. On the three calamitic special states (along the dashed lines) the subunit is cylindrically symmetric due to internal fluctuations. The subunit axis fluctuates and is on average oriented along the macroscopic optic axis. In the intermediate sectors A, B, and so on the subunit is orthorhombic and its external fluctuations create a macroscopic cylindrically symmetric state.

with the effective molecular symmetry). As shown in Fig. 6(b) the subunit form can be obtained by freezing any cylindrically symmetric subunit of the special states. Its orthorhombic symmetry results only from the up-down reversal process which cancels the molecular polarization without changing its dielectric and optic tensors. Let us remark that there are three different uniaxial subunits while there is a single biaxial one. The three uniaxial subunits have different (but isomorphic) effective groups with their continuous rotation axes parallel to X, Y , or Z , respectively.

In order to describe the distribution P in the general case, let us focus on its maxima. Figure 7 represents the most likely orientation of the subunit in the plane η_0, η'_0 . In the calamitic special state (i) the subunit is cylindrical and its symmetry axis Z fluctuates isotropically around the laboratory axis Oz . In the region denoted A, the orthorhombic subunit is also preferentially oriented with Z parallel to Oz . When Z is strictly parallel to Oz the orientation of the molecular plane YZ is completely disordered. However, when the direction of Z fluctuates out of Oz , the molecular plane takes a preferred orientation $\alpha=0$, i.e., the molecular axis Y stays in the tilt plane OzZ . In region F the disorder is similar, except for the preferred orientation of Y which is given by $\alpha=\pi/2$, i.e., Y is normal to the tilt plane. In regions B and C, which surround the calamitic state (ii), the most likely orientation is given by X parallel to Oz . When X fluctuates, Y is either parallel or normal to the tilt plane. In regions D and E, which surround the calamitic state (iii), the most likely orientation is given by Y parallel to OZ . When Y fluctuates, Z is either parallel or normal to the tilt plane.

Which one of the six configurations (CCD, etc.) is actually stabilized depends on the molecular shape and may change with temperature or concentration. It is evident that

for large opening angles the special state (iii) is favored with a DCD configuration. Similarly, the DDC special state (i) is favored at small opening angles. For micelles with edge lengths L_X, L_Y, L_Z satisfying $L_X \approx L_Y \ll L_Z$, the special state (ii) is favored with a CDD configuration. On the contrary, for very anisotropic molecules or close to the stability domain of the isotropic liquid, where fluctuations are quite large, no special state should be systematically stabilized.

IV. THE UNCONVENTIONAL BIAxIAL PHASE

The proper directions of the two tensors are parallel to the laboratory axes x, y, z in six equivalent domains of the biaxial phase. In these domains the distribution P ,

$$P(\alpha, \beta, \gamma) = P_0 + \eta_0 \frac{3\cos^2\beta - 1}{2} + \eta'_0 \frac{\sqrt{3}}{2} \sin^2\beta \cos 2\alpha + \eta_2 \frac{\sqrt{3}}{2} \sin^2\beta \cos 2\gamma + \eta'_2 \left(\cos 2(\alpha + \gamma) \cos^4 \frac{\beta}{2} + \cos 2(\alpha - \gamma) \sin^4 \frac{\beta}{2} \right) \quad (7)$$

depends on four independent parameters $\eta_0 = \eta_{0,0}$, $\eta_2 = \sqrt{2}\eta_{2,0}$, $\eta'_0 = \sqrt{2}\eta_{0,2}$, $\eta'_2 = 2\eta_{2,2}$. The uniaxial distribution [Eq. (5)] is obtained by setting $\eta_2 = \eta'_2 = 0$ whereas the standard biaxial nematic phase [Eq. (2)] corresponds to $\eta'_0 = \eta'_2 = 0$. The corresponding partial distributions read

$$P_Z(\theta_Z, \phi_Z) = P_0 + \eta_0 \frac{3\cos^2\theta_Z - 1}{2} + \eta_2 \frac{\sqrt{3}}{2} \cos 2\phi_Z \sin^2\theta_Z, \\ P_Y(\theta_Y, \phi_Y) = P_0 + \left(-\frac{1}{2}\eta_0 - \frac{\sqrt{3}}{2}\eta'_0 \right) \frac{3\cos^2\theta_Y - 1}{2} + \left(-\frac{1}{2}\eta_2 - \frac{\sqrt{3}}{2}\eta'_2 \right) \frac{\sqrt{3}}{2} \cos 2\phi_Y \sin^2\theta_Y, \\ P_X(\theta_X, \phi_X) = P_0 + \left(-\frac{1}{2}\eta_0 + \frac{\sqrt{3}}{2}\eta'_0 \right) \frac{3\cos^2\theta_X - 1}{2} + \left(-\frac{1}{2}\eta_2 + \frac{\sqrt{3}}{2}\eta'_2 \right) \frac{\sqrt{3}}{2} \cos 2\phi_X \sin^2\theta_X. \quad (8)$$

Each one exhibits the conventional biaxial form [Eq. (2)] and can thus be represented by a vector in the η_0, η_2 plane [Fig. 8(a)]. The components of the three corresponding vectors are

$$\begin{pmatrix} \eta_0 \\ \eta_2 \end{pmatrix} \text{ for } P_Z, \begin{pmatrix} -\eta_0/2 - \sqrt{3}\eta'_0/2 \\ -\eta_2/2 - \sqrt{3}\eta'_2/2 \end{pmatrix} \text{ for } P_Y, \\ \text{and } \begin{pmatrix} -\eta_0/2 + \sqrt{3}\eta'_0/2 \\ -\eta_2/2 + \sqrt{3}\eta'_2/2 \end{pmatrix} \text{ for } P_X.$$

They have different lengths and their orientations are only limited by the fact that their sum vanishes. Another set of three vectors representing an equivalent domain of the same structure is obtained after either a three fold rotation or a

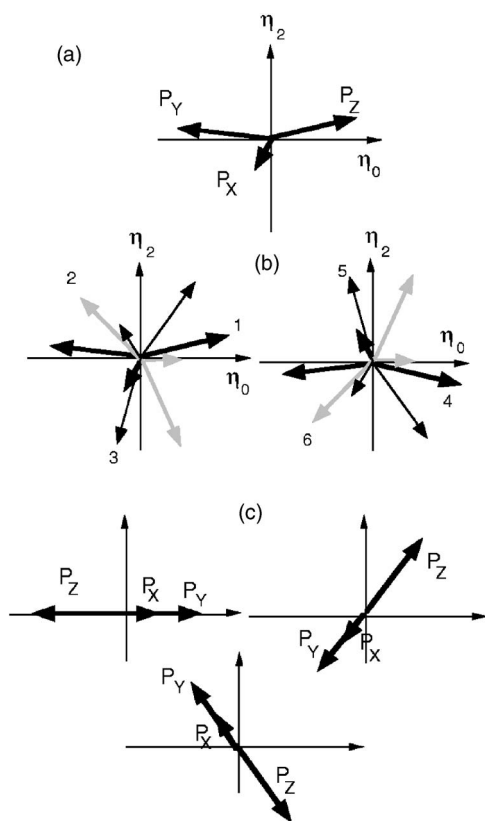


FIG. 8. (a) Star representing an unconventional biaxial state in the order-parameter space. Each branch describes one of the molecular axes X, Y , and Z . The statistical meaning of each branch is given in Fig. 1. (b) The six domains of the state (1) depicted in (a). Domains 2 and 3 result from 1 after three fold rotations around the direction (111) (i.e., permutations zxy and yzx of the laboratory axes). Domains 4, 5, and 6 result from mirror symmetries (yxz , etc.). (c) Three stars associated with the uniaxial phase.

planar symmetry in the η_0, η_2 plane. The six domains associated with a given state are represented in Fig. 8(b). When the three vectors are all horizontal (or all turned to $\pm 2\pi/3$) the phase is uniaxial [Fig. 8(c)]. The modulus of a given vector indicates the degree of ordering of the corresponding axis.

The classification of the uniaxial configurations with respect to their C or D character does not apply to biaxial configurations because there exists a single conventional biaxial state, which varies continuously between C and D. However for bent-core molecules the three vectors P_X, P_Y , and P_Z can lie inside different sectors B_1, B_2, \dots, B_6 of Fig. 1, yielding 21 biaxial non equivalent configurations. (a) In a first class of three configurations [Fig. 9(a)], two vectors belong to the same sector (e.g., X, Y in B_1) whereas the third vector belongs to the opposite sector (e.g., Z in B_4). The molecular axes X and Y are oriented along Oz and fluctuate preferentially in the Oxz plane whereas Z is oriented along Oy and fluctuates in Oxy . The two additional configurations belonging to this class result from circular permutations of the molecular indices X, Y , and Z . (b) In a second class [Fig. 9(b)] of six configurations, Y is in B_6 . This configuration is quite similar to (a) except that the preferential fluctuations of

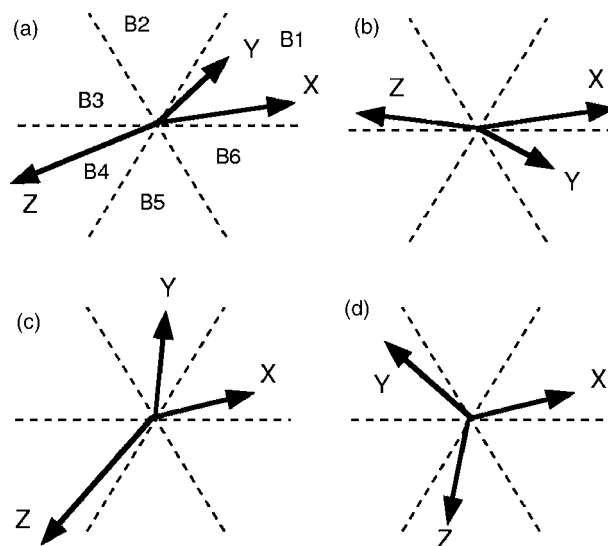


FIG. 9. Classes of distinct unconventional biaxial states.

Y are now normal to those of X . The mean direction of Z can be either Ox (Z in B_3) or Oy (Z in B_4). (c) In the third class [Fig. 9(c)] two vectors belong to two adjacent sectors (B_1 and B_2) whereas the third vector is in a non adjacent sector (B_4 or B_5). X is on average parallel to Oz , Y to Ox , and Z to Oy . The plane of preferred fluctuations is the same for X and Y (Oxz). Five permutations of X, Y, Z provide the other configurations of the class. (d) In the fourth class [Fig. 9(d)], the three vectors belong to non adjacent sectors (B_1, B_3, B_5). Their mean orientations are perpendicular and they fluctuate in three perpendicular planes.

In (a) and (b) two molecular axes are macroscopically parallel, indicating for instance a rotation of the molecule around the internal axis $X+Y$ [Fig. 5(c)]. Contrariwise, when one neglects the fluctuations in the configurations (c) and (d) the subunit has a well-defined mean orientation provided that the three vectors are almost calamitic [i.e., close to the axes denoted $C(z), C(y)$, and $C(x)$ in Fig. 1]. The molecular axes are then on average parallel to the laboratory axes. When one or several vectors are almost diskotic the situation is less simple. When the three vectors are diskotic, the three molecular axes participate in the ordering along each laboratory axis. P is thus associated with a mixture of subunits with their main axes X, Y, Z oriented parallel to x, y, z, z, x, y , and y, z, x , respectively.

Three families of conventional special states are stabilized when the subunit becomes cylindrically symmetric. In the first family ($\eta'_0 = \eta'_2 = 0$) P coincides with [Eq. (2)] where the role of the molecular long axis is played by the symmetry axis Z of the double-cone subunit depicted in Fig. 6(a) state (i). All the states in this family have the configuration (a) with

$$P_X = P_Y = \begin{pmatrix} -\eta_0/2 \\ -\eta_2/2 \end{pmatrix}$$

and

$$P_Z = \begin{pmatrix} \eta_0 \\ \eta_2 \end{pmatrix}$$

. Although the subunit is then cylindrically symmetric around Z , the axes Y and X have a common well-defined mean orientation. The distribution coincides with the uniaxial special states DDC ($\eta_0 > 0$) and CCD ($\eta_0 < 0$) when $\eta_2 = 0$. In the two other families, which are obtained after circular permutations of X, Y , and Z , the subunit takes the form of a flat disk or of a curved cylinder presented in Fig. 6(a) states (iii) and (ii).

V. THERMODYNAMICS OF THE UNIAXIAL PHASE

The thermodynamic complexity of the liquid \rightarrow nematic transition is dramatically increased by the presence of a second tensor. Indeed, the order-parameter space contains now seven effective components instead of two within the one-tensor model. The corresponding free energy can be written as a polynomial function of ten basic invariants I_1, I_2, \dots, I_{10} , instead of only two, I_1 and I_4 , for conventional nematics. Their maximal degree is nine and the ten invariants are related by three algebraic relations (siszygies). For example, the three second-degree invariants are

$$\begin{aligned} I_1 &= \eta_0^2 - 2\eta_1\eta_{-1} + 2\eta_2\eta_{-2}, \\ I_2 &= \eta_0'^2 - 2\eta_1'\eta_{-1}' + 2\eta_2'\eta_{-2}', \\ I_3 &= \eta_0\eta_0' - \eta_1\eta_{-1}' - \eta_{-1}\eta_1' + \eta_2\eta_{-2}' + \eta_{-2}\eta_2'. \end{aligned} \quad (9)$$

To stabilize all the ordered phases F must be expanded to the degree 18. We will not attempt to perform an extensive thermodynamic analysis based on this very complex potential. Instead, let us focus on the isotropic \rightarrow uniaxial transition which can be described with a fourth-degree expansion. Since in the uniaxial nematic phase only two order-parameter components η_0 and η_0' are not equal to zero, the free energy takes the simplified form

$$\begin{aligned} F_u &= a\eta_0^2 + b\eta_0^3 + c\eta_0^4 + a'\eta_0'^2 + b'\eta_0'^3 + c'\eta_0'^4 + e\eta_0\eta_0' \\ &+ d\eta_0^2\eta_0'^2 + f\eta_0\eta_0'^3 + g\eta_0^3\eta_0' + h\eta_0\eta_0'^2 + i\eta_0^2\eta_0' \end{aligned} \quad (10)$$

where a, b, \dots are phenomenological coefficients which depend smoothly on external fields (temperature, concentration, etc.) and on molecular parameters (opening angle, etc.). c and c' are positive and d is larger than a critical value $d_c(f, g)$ [with $d_c(f, g) \geq 2|f+g|-1$, the equality holding only for $f=g=0$]. One can see by inspecting the equations of state

$$\begin{aligned} \frac{\partial F_u}{\partial \eta_0} &= 2a\eta_0 + 3b\eta_0^2 + 4c\eta_0^3 + e\eta_0' + 2d\eta_0\eta_0'^2 + h\eta_0'^2 + 2i\eta_0\eta_0' \\ &+ f\eta_0'^3 + 3g\eta_0^2\eta_0' = 0, \end{aligned}$$

$$\begin{aligned} \frac{\partial F_u}{\partial \eta_0'} &= 2a'\eta_0' + 3b'\eta_0'^2 + 4c'\eta_0'^3 + e\eta_0 + 2d\eta_0^2\eta_0' + i\eta_0^2 \\ &+ 2h\eta_0\eta_0' + 3f\eta_0^2\eta_0' + g\eta_0^3 = 0, \end{aligned} \quad (11)$$

that there is no equilibrium solution with a single nonzero

order parameter. Indeed, putting $\eta_0=0$ in Eqs. (11) yields $\eta_0'=0$, except at exceptional positions in the phase diagram, defined by $e(4c'h-3b'f)^2 + h(2a'f-4c'e)(4c'h-3b'f) + f(2a'f-4c'e)^2 = 0$.

Minimizing F_u with respect to η_0 and η_0' yields a variety of topologically distinct phase diagrams. They are all comprised of a single first-order isotropic-nematic transition line together with a set of isostructural (liquid-gas type) lines. The topology of the isostructural network depends on the effective coupling coefficients $\delta = d/\sqrt{cc'}$ and $\varepsilon = (4/3)^2 e/bb'\sqrt{cc'}$ whereas its symmetry depends on the ‘‘asymmetric ratios’’ $s_1 = (b/b')^2$, $s_2 = (g/f)\sqrt{(c'/c)s_1}$ and $s_3 = (i/h)\sqrt{s_2(f/g)}$. For unit value of s_1, s_2 , and s_3 the phase diagrams are symmetric with respect to the permutation of the coefficients $\alpha = 8a/9b^2\sqrt{c}$ and $\alpha' = 8a'/9b'^2\sqrt{c'}$. In the general case, only the quadratic coefficients depend strongly on temperature and the relevant phase diagram is in the α - α' - ε space. However, for simplicity, the various phase diagrams presented in Fig. 10 are drawn in the α - α' plane, assuming also a constant value for ε .

The simplest phase diagram [Fig. 10(a)] arises when δ and ε are small and positive. Below the isotropic-nematic line (I - N), the nematic stability domain is cut into two pieces separated by a first-order isostructural transition line which intersects I - N at a triple point T_1 . This line terminates at a second triple point T_2 where it splits into two isostructural lines. No critical point appears at the end of these lines so that three apparently distinct uniaxial nematic phases are stabilized in this diagram. The first one, denoted N , is stabilized when α becomes negative while α' remains positive [pathway pw1 in Fig. 10(a)]. Close to the transition line and far from T_1 , η_0 is negative and η_0' is small and positive when b and b' are positive. The corresponding nematic configuration is CCD whereas it is DDC when b is negative. Analogously, when α' becomes negative η_0' is negative ($b' > 0$) and η_0 is small. The corresponding distribution is associated with the configuration pictured in sector E of Fig. 7 (sector B for $b' < 0$). When f, g, h , and i are small and the asymmetric ratios are close to unity, these configurations remain stable in the whole domains N and N' . The $N \rightarrow N'$ transition is then strongly first order. In the middle of the third stability zone, the order-parameter components in the corresponding ‘‘phase’’ N_e are negative ($s_1, s_2, s_3 \approx 1$ and $b, b' > 0$) and have similar magnitudes. The molecules are then oriented as in sector D of Fig. 7. On approaching the isostructural lines, one of the components decreases and the representative point in Fig. 7 moves toward C or E . For larger values of f, g, h, i , and of the asymmetric ratios, no simple general rule can be given for relating the phases N, N_e , and N' to specific configurations described in Figs. 5 and 7.

For negative values of ε , one predicts a similar phase diagram [Fig. 10(b)], except that the isostructural lines have critical end points T_c and T_c' . Along a thermodynamic pathway (pw3) bypassing T_c and T_c' , the system continuously modifies its molecular structure between, e.g., CCD and $E(b, b' > 0)$. When δ is negative, a direct transition from the isotropic liquid to the ‘‘phase’’ N_e is possible and new triple points appear at the intersection between I - N and the isostructural lines. When $\varepsilon < 0$ the isostructural lines have criti-

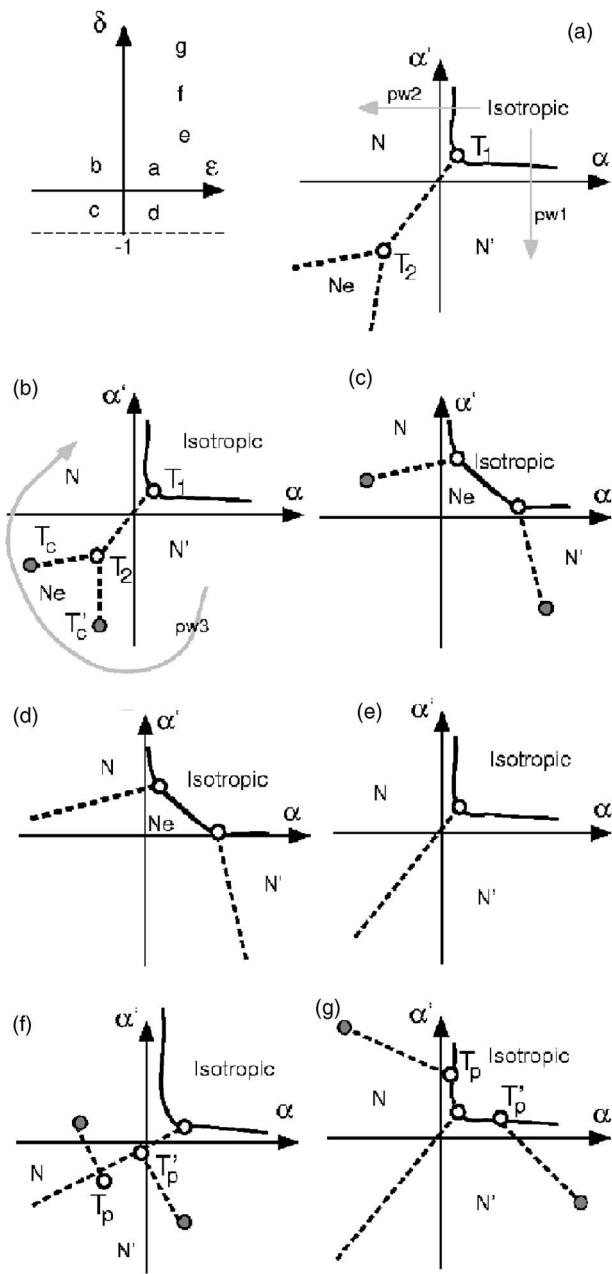


FIG. 10. Phase diagrams resulting from the minimization of F_u [Eq. (11)] for various values of the coefficients ϵ and δ . The continuous lines represent the symmetry breaking first-order transition from the isotropic liquid to the nematic phase. Dashed lines represent isostructural first-order transitions. $T_1, T_2, T_p,$ and T'_p are triple points. T_c and T'_c are critical points occurring at the end of isostructural transition lines. $N, N',$ and Ne are different states of the uniaxial nematic phase. All the diagrams [except (f)] correspond to small values of the coefficients f, g, h, i in Eq. (11) and almost unit values of the asymmetric ratios.

cal points [Fig. 10(c)] while these points are thrown back to infinity when ϵ becomes positive [Fig. 10(d)]. When both ϵ and δ are large and positive, a single isostructural line, without critical point, is present in the phase diagram [Fig. 10(e)]. Ne is then nowhere stable. For still larger values of δ, N and N' are also split by isostructural transitions with critical points [Fig. 10(f)]. These lines meet the main isostructural

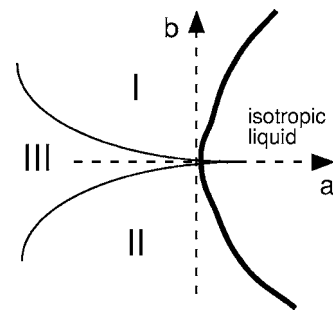


FIG. 11. Theoretical phase diagram obtained for systems invariant under the permutation of the molecular axes X, Y, Z . a and b are the phenomenological coefficients below the second- and third-order invariants in the free energy. I, II, and III are the stability domains of the three uniaxial phases which differ by their internal symmetries. I and II have cylindrical internal symmetry groups and coincide with the special states CDC, DCC, CCD and DDC, DCD, CDD, respectively. III has the orthorhombic internal symmetry D_{2h} . The four phases merge into a single Landau point for $a=b=0$. This diagram is the internal analog of the conventional phase diagram associated with the isotropic \rightarrow uniaxial (I=calamitic, II=diskotic) \rightarrow biaxial (III) transitions.

transition line at triple points T_p and T'_p . On still increasing δ , the triple points T_p and T'_p move toward the isotropic phase and finally arrive on the isotropic-nematic transition [Fig. 10(g)].

By choosing the asymmetric ratios close to unity, we have singled out the molecular Z axis. We can of course foresee similar diagrams after permuting the axes X, Y, Z , i.e., by applying internal operations in the space of the phenomenological parameters a, a', \dots . For instance the identification of N with CCD ($b > 0$) in the $a-a'-e$ diagram is thus replaced by CDC in the $a_1-a'_1-e_1$ diagram when $b_1 > 0$ (a_1, a'_1, e_1 , and b_1 being the images of a, a', e , and b under an internal three fold rotation).

Consider finally a system in which the free energy is invariant under the permutation of the three molecular axes. This case represents a fair approximation for almost cubic micelles. The five invariants appearing in F_u are then replaced with only two invariants $\eta_0^2 + \eta_0'^2$ and $\eta_0^3 - 3\eta_0\eta_0'^2$ and the phenomenological coefficients are related by $a=a', h=-3b, c=c'=d/2$, and $b'=f=g=i=e=0$. The corresponding phase diagram associated with a sixth-degree expansion is given in Fig. 11. In sector I of this diagram the three special states CCD, CDC, and DCC coexist (they are energetically equivalent domains of a single phase) whereas in sector II the special states DDC, DCD, and CDD coexist. Second-order transition lines separate these sectors from sector III in which six domains of the general uniaxial nematic configuration coexist. This diagram is the “internal analog” of the conventional isotropic-uniaxial-biaxial phase diagram [7]. In the realistic situation when $b', f, g, a-a', h+3b, \dots$ are finite but small, the second-order transitions disappear and a single domain becomes more stable at each point in the phase diagram. The set of isostructural transitions between these “domains” forms an intricate network, the form of which depends on the values of the small coefficients. A similar analysis can be carried out for almost quadratic mol-

ecules or micelles in which, for instance, CDD is a distinguished phase whereas DCD and DDC are two equivalent domains of another phase.

Let us notice that although no isostructural transition has yet been reported in bent-core systems, Nounesis *et al.* [18] have observed an isostructural transition with a critical point in binary mixtures of long-core polar liquid crystals, interpreted by the authors within another theoretical context.

VI. ORDER-PARAMETER MEASUREMENTS

Let us now justify the two tensors at the microscopic level. The mesogen symmetry C_{2v} permits the existence of two independent *microscopic* traceless second-rank tensors $\Omega_{(0)}$ and $\Omega_{(2)}$ rigidly tied to the molecule. Indeed, its orthorhombic symmetry allows the molecule to carry only diagonal (traceless) tensors Ω which can be expanded, on the molecular frame X, Y, Z , as

$$\hat{\Omega} = \begin{pmatrix} \Omega_{XX} & & \\ & \Omega_{YY} & \\ & & -\Omega_{XX} - \Omega_{YY} \end{pmatrix} \\ = \frac{\Omega_{XX} + \Omega_{YY}}{\sqrt{2/3}} \Omega_{(0)} + \frac{\Omega_{XX} - \Omega_{YY}}{2} \Omega_{(2)},$$

$$\Omega_{(0)} = \frac{1}{\sqrt{6}} \begin{pmatrix} 1 & & \\ & 1 & \\ & & -2 \end{pmatrix}, \quad \Omega_{(2)} = \begin{pmatrix} 1 & & \\ & -1 & \\ & & 0 \end{pmatrix}. \quad (12)$$

η and η' are related to $\langle \Omega_{(0)} \rangle$ and $\langle \Omega_{(2)} \rangle$ $\langle \Omega \rangle$ means averaging Ω over the statistical distribution $P(\alpha, \beta, \gamma)$. The matrix elements of $\Omega_{(0)}$ and $\Omega_{(2)}$ in Eq. (12) are constant whereas their proper directions X, Y, Z depend on α, β, γ . In the isotropic liquid phase the fluctuations are isotropic and one finds $\langle \Omega_{(0)} \rangle = \langle \Omega_{(2)} \rangle = 0$. In contrast, in the triclinic (C_i) phase all the Cartesian components of $\langle \Omega_{(0)} \rangle$ and $\langle \Omega_{(2)} \rangle$ are finite in the laboratory frame x, y, z .

In the biaxial phase only diagonal components of $\langle \Omega_{(0)} \rangle$ and $\langle \Omega_{(2)} \rangle$ take finite values in the laboratory frame. Using Eq. (4) to perform the statistical average yields

$$\langle \Omega_{(0)} \rangle = \frac{16\pi^2}{5\sqrt{2}} \begin{pmatrix} \eta_2 - \frac{\eta_0}{\sqrt{3}} & & \\ & -\eta_2 - \frac{\eta_0}{\sqrt{3}} & \\ & & \frac{2}{\sqrt{3}} \eta_0 \end{pmatrix},$$

$$\langle \Omega_{(2)} \rangle = \frac{16\pi^2}{10} \begin{pmatrix} \eta_2' - \frac{\eta_0'}{\sqrt{3}} & & \\ & -\eta_2' - \frac{\eta_0'}{\sqrt{3}} & \\ & & \frac{2}{\sqrt{3}} \eta_0' \end{pmatrix}, \quad (13)$$

where the matrix elements $\langle \Omega_{(q)} \rangle_{ij}$ in Eq. (13) are taken over the laboratory indices $i, j = x, y, z$ [while $I, J = X, Y, Z$ in Eq. (12)]. Consider now two macroscopic physical tensors $\langle \varepsilon \rangle$ and $\langle \mu \rangle$ which are the mean values of the molecular quantities ε and μ , for instance, the dielectric and magnetic susceptibilities, the optic tensor at two different frequencies, or the electric and magnetic quadrupolar moments. Suppose that $\varepsilon_{XX}, \varepsilon_{YY}, \varepsilon_{ZZ}, \mu_{XX}, \mu_{YY}$, and μ_{ZZ} are known from independent measurements or microscopic calculations. Their traceless parts can be written as in Eq. (12):

$$\varepsilon - \frac{\text{Tr } \varepsilon}{3} = \frac{\varepsilon_{XX} + \varepsilon_{YY} - 2\varepsilon_{ZZ}}{\sqrt{6}} \Omega_{(0)} + \frac{\varepsilon_{XX} - \varepsilon_{YY}}{2} \Omega_{(2)}, \\ \mu - \frac{\text{Tr } \mu}{3} = \frac{\mu_{XX} + \mu_{YY} - 2\mu_{ZZ}}{\sqrt{6}} \Omega_{(0)} + \frac{\mu_{XX} - \mu_{YY}}{2} \Omega_{(2)}. \quad (14)$$

Averaging Eqs. (14) and combining with Eqs. (13) yields the set of linear equations

$$\frac{5}{48\pi^2} (2\langle \varepsilon \rangle_{xx} - \langle \varepsilon \rangle_{yy} - \langle \varepsilon \rangle_{zz}) \\ = \frac{\varepsilon_{XX} + \varepsilon_{YY} - 2\varepsilon_{ZZ}}{2\sqrt{3}} \left(\eta_2 - \frac{\eta_0}{\sqrt{3}} \right) + \frac{\varepsilon_{XX} - \varepsilon_{YY}}{4} \left(\eta_2' - \frac{\eta_0'}{\sqrt{3}} \right), \\ \frac{5}{48\pi^2} (2\langle \varepsilon \rangle_{yy} - \langle \varepsilon \rangle_{xx} - \langle \varepsilon \rangle_{zz}) \\ = \frac{\varepsilon_{XX} + \varepsilon_{YY} - 2\varepsilon_{ZZ}}{2\sqrt{3}} \left(-\eta_2 - \frac{\eta_0}{\sqrt{3}} \right) \\ + \frac{\varepsilon_{XX} - \varepsilon_{YY}}{4} \left(-\eta_2' - \frac{\eta_0'}{\sqrt{3}} \right), \\ \frac{5}{48\pi^2} (2\langle \mu \rangle_{xx} - \langle \mu \rangle_{yy} - \langle \mu \rangle_{zz}) \\ = \frac{\mu_{XX} + \mu_{YY} - 2\mu_{ZZ}}{2\sqrt{3}} \left(\eta_2 - \frac{\eta_0}{\sqrt{3}} \right) + \frac{\mu_{XX} - \mu_{YY}}{4} \left(\eta_2' - \frac{\eta_0'}{\sqrt{3}} \right), \\ \frac{5}{48\pi^2} (2\langle \mu \rangle_{yy} - \langle \mu \rangle_{xx} - \langle \mu \rangle_{zz}) \\ = \frac{\mu_{XX} + \mu_{YY} - 2\mu_{ZZ}}{2\sqrt{3}} \left(-\eta_2 - \frac{\eta_0}{\sqrt{3}} \right) \\ + \frac{\mu_{XX} - \mu_{YY}}{4} \left(-\eta_2' - \frac{\eta_0'}{\sqrt{3}} \right), \quad (15)$$

the solution of which provides the order-parameter components η_0, η'_0, η_2 , and η'_2 as functions of the experimentally determined microscopic $\varepsilon_{XX}, \varepsilon_{YY}, \varepsilon_{ZZ}, \mu_{XX}, \mu_{YY}, \mu_{ZZ}$ and macroscopic $\langle \varepsilon \rangle_{xx}, \langle \varepsilon \rangle_{yy}, \langle \varepsilon \rangle_{zz}, \langle \mu \rangle_{xx}, \langle \mu \rangle_{yy}, \langle \mu \rangle_{zz}$ quantities.

Direct measurements of $\langle \Omega_{(0)} \rangle$ and $\langle \Omega_{(2)} \rangle$ can also be completed by means of diffusion experiments. Inserting the orthogonality relations of the Euler functions [16] in Eq. (4) leads to the following definitions for η and η' : $\eta_{m,0} = (5/16\pi^2) \langle D_{m,0}^2 \rangle$, $\eta'_{m,2} = (5/16\pi^2) \langle D_{m,2}^2 \rangle = (5/16\pi^2) \langle D_{m,-2}^2 \rangle$. In the uniaxial and biaxial phases they become

$$\begin{aligned}\eta_0 &= \frac{5}{32\pi^2} \langle 3\cos^2\beta - 1 \rangle, \\ \eta_2 &= \frac{5\sqrt{3}}{32\pi^2} \langle \cos 2\gamma \sin^2\beta \rangle, \\ \eta'_0 &= \frac{5\sqrt{3}}{32\pi^2} \langle \cos 2\alpha \sin^2\beta \rangle, \\ \eta'_2 &= \frac{5}{16\pi^2} \left\langle \cos 2(\alpha + \gamma) \cos^4 \frac{\beta}{2} + \cos 2(\alpha - \gamma) \sin^4 \frac{\beta}{2} \right\rangle.\end{aligned}\quad (16)$$

These coefficients, which are denoted S_1, S_2, S_4 , and S_5 , respectively in Ref. [19], can be measured for instance by quadrupolar nuclear magnetic resonance on spinning samples [19] or other NMR experiments [20]. A number of classical techniques, neutron and x-ray diffusion, Raman spectroscopy and so on can also evaluate these parameters.

η_0, η'_0, η_2 , and η'_2 permit one to evaluate quantitatively the degree of biaxiality of the actual state of the system at both macroscopic (external) and microscopic (internal) points of view. The external and internal ‘‘biaxiality coefficients’’

$$\begin{aligned}B_{\text{ext}} &= \frac{\eta_2^3 - 3\eta_2\eta_0^2}{(\eta_0^2 + \eta_2^2)^{3/2}}, \\ B_{\text{int}}^{(0)} &= \frac{\eta_0^3 - 3\eta_0'\eta_2^2}{(\eta_0'^2 + \eta_2'^2)^{3/2}}\end{aligned}\quad (17)$$

vanish in the special uniaxial states where the internal and external groups are both cylindrically symmetric. B_{ext} is finite in the biaxial phase and vanishes as $(T - T_C)^{1/2}$ close to the biaxial \rightarrow uniaxial transition temperature T_C . B_{int} vanishes only in the special uniaxial or biaxial states. In general B_{int} is finite in the uniaxial phase (except in the special states) whereas B_{ext} remains finite even in the special states of the biaxial phase. Since the special states have no extended domains of stability in the phase diagram, B_{int} may be very small but never strictly zero. B_{ext} could be defined as well as $B_{\text{ext}}' = (\eta_2^3 - 3/2\eta_2\eta_0'^2)/(\eta_0'^2 + \eta_2'^2)^{3/2}$ and B_{int} as $B_{\text{int}}^{(2)} = \eta_2'^3 - 3\eta_2'\eta_2'^2/(\eta_2'^2 + \eta_2^2)^{3/2}$ which vanish under the same conditions as B_{ext} and $B_{\text{int}}^{(0)}$.

VII. DISCUSSION

Numerical simulations by Lansac *et al.* [4] predict the stabilization of the nematic phase for bent-core molecules with an opening angle larger than 135° , i.e., larger than the opening angle of the majority of the studied molecules. Dingemans *et al.* [21] observed a high-temperature nematic phase with hockey-stick-shaped mesogens bent to 132° and bent-core mesogens with opening angle larger than 140° . On the other hand, bent-core mesogens give rise to nematics in mixtures with stick like molecules. Pratibha *et al.* have observed a uniaxial nematic phase [5] above various smectic structures for mixtures with concentrations in bent-core molecules smaller than 35%. By studying the molecular orientation in the smectic phases which onset just below the nematic, they found three distinct behaviors. At low concentration c , a smectic- A_2 (Sm- A_2) phase is stabilized with Z parallel to the optic axis. Increasing c yields first an ordering of the bent-core molecules in a biaxial Sm- A_{2b} configuration and then a reorientation of Z in a direction normal to the optic axis, leading to the formation of the $B6$ antiferroelectric structure. The interpretation of the experimental data by the authors is given in terms of a single molecular orientation and does not permit one to determine the order-parameter values and the exact form of the distribution. However, since the observed transitions are weakly first order, the variation of P must almost be continuous between the three previous molecular orientations and corresponds to a long connected path in the order-parameter space $\eta_0, \eta'_0, \eta_2, \eta'_2$. The experimental data are not sufficient to follow the transformations of the order parameter, but it is evident that along this path the system necessarily crosses configurations (as, e.g., the ‘‘diskotic’’ DCC special state) in which the fluctuations prevent the formation of states where all the molecules are similarly oriented. More specifically, in the contiguous nematic phase we may tentatively assume that the molecular order is close to that in the neighboring smectic phases. Close to the transitions, the local biaxial or polar character of Sm- A_{2b} and $B6$ is then a small perturbation of the uniaxial molecular ordering in the nematic. Hence, the preceding transformations in the smectic phases correspond in the nematic to a continuous evolution from DDC to DCD, i.e., a $2\pi/3$ rotation in the η_0, η'_0 plane. At intermediate concentrations, corresponding to the biaxial smectic region, the nematic distribution reaches states in which one cannot assign a definite orientation to the subunit axes (P_Y and then P_Z becoming even isotropic at given concentrations) on the one hand and the special state (ii) in the diskotic DCC configuration on the other hand. The molecular orientation in this latter state is rather complex for the subunit has a flat-disk shape [Fig. 6(a)] with its axis X precessing isotropically around the macroscopic optic axis.

Pure bent-core nematic phases were first evidenced by Matraszek *et al.* [22]. Wirth *et al.* [23], have observed a uniaxial phase stabilized above a smectic- A phase in a compound of molecules with short terminal chains. Weissflog *et al.* [24], have shown that the nematic is stabilized only for molecules with opening angles larger than 165° . Such molecules are almost stick like and one expects they follow a conventional nematic behavior. Stodanijovic *et al.* [25] have

studied the dynamic light scattering by a uniaxial nematic phase in a pure bent-core system with rather small opening angle (120°). They found the long molecular axis Y along the optic axis (DCD) and anomalous physical behaviors indicating that the molecule is strongly bent. The order-parameter fluctuations have been studied within the framework of a model taking into account one second-rank tensor and one vector (polarization). Since C_{2v} molecules permit a single vector but two tensors, we think the data interpretation should be improved by taking into account a second tensor. Similar measurements have been carried out by Olivares *et al.* [26] in a compound with larger opening angle (140°). They found an uniaxial phase becoming biaxial under electric-field application. In this system the anomalies are not present. We argue that in this case the distribution is almost conventional and P is quite close to the special state (iii) in the DCD configuration. The main order parameter is then $\omega_0 = -(1/2)\eta_0 - (\sqrt{3}/2)\eta'_0$ and the corrections are proportional to the small secondary tensor $\omega'_0 = -(1/2)\eta'_0 - (\sqrt{3}/2)\eta_0$.

The possibility of stabilizing the biaxial nematic phase in bent-core systems was first suggested by numerical simulations [27]. In order to confirm this prediction Dingemans and Samulski [28] observed the Schlieren texture of the nematic phase in ODBP (2,5-bis (p-hydroxyphenyl)-1,3,4-oxadiazole). This texture, which is characterized by the absence of four-branch disclinations, exhibits biaxial features. The biaxiality was confirmed by Acharya *et al.* [29] who analyzed the four-peak x-ray pattern under electric field for ODBP molecules with opening angle 140° . Evidence of a biaxial phase was reported by Madsen *et al.* [5] from electro-optic and conoscopic measurements in the same system. Using NMR spectroscopy, they provided the first unambiguous confirmation of a biaxial nematic phase in a thermotropic liquid crystal.

Biaxial and uniaxial nematic phases have recently been reported with tetrapode mesogens [30]. The authors state that they form quasi platelet objects with an orthorhombic group. The four order-parameter components have been measured by infrared absorbance experiments. They are denoted S ($=\eta_0 16 \pi^2/5$), D ($=\eta'_0 16 \pi^2 \sqrt{3}/5$), P ($=\eta_2 16 \pi^2 \sqrt{3}/5$), and C ($=\eta'_2$). At 280 K the biaxial coefficients [Eqs. (17)] are large: $B_{\text{ext}} = -0.75$, $B'_{\text{ext}} = -0.57$, $B_{\text{int}(0)} = -0.47$, $B_{\text{int}(2)} = -1$. The values of the three partial distributions [Eq. (8)] (up to a common numerical factor)

$$P_Z = \begin{pmatrix} 0.7 \\ 0.2 \end{pmatrix}, \quad P_Y = \begin{pmatrix} -0.46 \\ -0.21 \end{pmatrix}, \quad P_X = \begin{pmatrix} -0.24 \\ 0.01 \end{pmatrix},$$

show that Z is in $B1$, Y in $B4$, and X in $B3$, i.e., the molecular ordering is of type c [Fig. 9(c)]. The three molecular axes are oriented on average along the three perpendicular laboratory directions with strong fluctuations for the axis X . On approaching the uniaxial transition, B_{ext} and $B_{\text{int}(0)}$ decrease to about -0.1 , indicating a softening of both external and internal biaxialities. However, B'_{ext} and $B_{\text{int}(2)}$ remain large (≈ -1). In the uniaxial phase B_{ext} and B'_{ext} cancel whereas the internal biaxiality $B_{\text{int}(0)} = -0.15$ remains small. The corresponding molecular structure DDC is almost conventional.

In the biaxial phase the ratios S/D and P/C relating the first (η) and second (η') tensor components are about $1/3$ at low temperature and decrease on approaching the biaxial \rightarrow uniaxial transition. Since the two tensors have similar amplitudes, the cross coupling must be strong (one cannot distinguish primary and secondary order parameters). Then the fair agreement found in Ref. [30] with the one-tensor model of the biaxial phase [7,8] is certainly casual. In contrast, in the uniaxial phase the ratio S/D is about $1/10$ and η can be considered as an actual primary order parameter and η' as a secondary induced order parameter.

At first sight our approach holds also for lyotropic systems made with orthorhombic micelles. However, micelles are soft objects which change their shape with temperature or concentration and adapt their microscopic asymmetry to that of the medium [31]. In particular, the difference between the calamitic and diskotic uniaxial phases lies in a modification of the micellar shape and not in the modification of the orientational distribution of rigid objects. Accordingly, a realistic phenomenological treatment of lyotropic nematics needs at least three order parameters, namely, two second-rank tensors and one additional internal degree of freedom accounting for the shape changes. Such an internal parameter has been invoked [32], for instance, within the one-tensor model to explain the presence of two four-phase points observed in various lyotropic liquid crystals [31,33]. The second tensor destroys the qualitative difference between calamitic and diskotic structures and prevents the stabilization of a four-phase point in the phase diagram. Thus, we think that the theoretical situation remains quite unclear in lyotropic micellar systems. Whether the observation of a four-phase point results from inaccurate measurements in systems approximately described by the one-tensor model or from a stabilization effect of the internal degree of freedom is yet an open question. Let us finally notice that in the two-tensor theory of Straley [12], a four-phase point is predicted for orthorhombic molecules or micelles in contradiction with our results. It is only for rigid objects with symmetry group lower than orthorhombic that Straley claims the disappearance of the four-phase point. The disappearance of this point has also been theoretically predicted by Chrzanowska [34] in mixtures of rodlike and disklike particles, but only for a limited range of the microscopic parameters.

ACKNOWLEDGMENT

I acknowledge helpful discussions with Professor V. Lorman.

APPENDIX

$P(\alpha, \beta, \gamma)$ can be formally rewritten as a function $P(R_{\alpha, \beta, \gamma})$ of the rotation matrix $R_{\alpha, \beta, \gamma}$ associated in the real space with the Euler angles α, β, γ . The actions of external and internal rotations on P are then defined by

$$\begin{aligned} (R_{abc}^{\text{ext}} P)(R_{\alpha\beta\gamma}) &= P(R_{abc}^{-1} R_{\alpha\beta\gamma}), \\ (R_{abc}^{\text{int}} P)(R_{\alpha\beta\gamma}) &= P(R_{\alpha\beta\gamma} R_{abc}^{-1}). \end{aligned} \quad (\text{A1})$$

Applying Eqs. (A1) on the 25 Euler functions D_{mp}^2 yields an irreducible representation of the direct product $O(3)^{\text{ext}} \otimes O(3)^{\text{int}}$:

$$R_{abc}^{\text{ext}} D_{nm}^2 = \sum_{p=-2}^2 D_{np}(R_{abc}^{-1}) D_{pm}^2,$$

$$R_{abc}^{\text{int}} D_{nm}^2 = \sum_{p=-2}^2 D_{pm}(R_{abc}^{-1}) D_{np}^2, \quad (\text{A2})$$

which shows that external and internal rotations act on the first (n) and second (m) indices of $\eta_{n,m}$, respectively. The distribution P is obviously invariant under the internal operations g belonging to the internal molecular group G^{int} : $gP = P$. The general invariant form of P can thus be found by applying the projector $\sum_{g \in G^{\text{int}}} g$ onto Eq. (3). Elementary matrix algebra leads then to Eq. (2) for uniaxial molecular groups $G^{\text{int}} = C_3, C_{3v}, D_4, \dots, D_{\infty h}$ and to Eq. (4) when $G^{\text{int}} = C_{2v}, D_2$, or D_{2h} . The average behavior of the molecules is the same within each series. This means in particular that all the uniaxial molecules spin symmetrically around their rotation axis to reach the effective molecular group $D_{\infty h}$ while in the orthorhombic series such rotation does not happen and the subunit remains, in general, orthorhombic.

The partial distributions presented in Eqs. (6) and (8) are calculated as follows. Let A be a unit vector within the molecule and g one of the internal rotation matrices transforming

Z into A : $A = g e_Z$. $P_A(\theta, \varphi)$ is the probability to find A along the direction defined by the spherical angles (θ, φ) in the laboratory frame. If we denote by $E(A)$ the set of molecular orientations (α, β, γ) such that A is fixed along (θ, φ) , then $P_A(\theta, \varphi) = \sum_{\alpha\beta\gamma \in E(A)} P(\alpha, \beta, \gamma)$. Let us first carry out the case $A = Z$. $E(Z) = \{(\alpha, \theta, \varphi) \text{ with } 0 \leq \alpha < 2\pi\}$ and $P_Z(\theta, \varphi) = \int_0^{2\pi} P(\alpha, \theta, \varphi) d\alpha$. After inserting Eq. (4) in this integral and using the orthogonality of the D_{mp}^L one finds

$$P_Z(\theta, \varphi) = 2\pi \sum_{m=-2}^2 \eta_{m,0} D_{m0}^2(\beta = \theta, \gamma = \varphi). \quad (\text{A3})$$

When $A \neq Z$ one defines a new molecular frame $(X_1, Y_1, Z_1) = g(X, Y, Z)$ (with $Z_1 = A$) and a new distribution function $P_1(\alpha_1, \beta_1, \gamma_1) = P(\alpha, \beta, \gamma)$ where $\alpha_1, \beta_1, \gamma_1$ are the Euler angles of the new frame when α, β, γ are those of the former frame: $P_1(R_{\alpha_1, \beta_1, \gamma_1}) = P(R_{\alpha, \beta, \gamma} g^{-1})$. One determines $P_A(\theta, \varphi) = \int_0^{2\pi} P_1(\alpha_1, \theta, \varphi) d\alpha_1$ by inserting Eq. (4) in this integral and by using Eq. (A2) and the orthogonality of the D_{mp}^L :

$$P_A(\theta, \varphi) = 2\pi \sum_{m=-2}^2 D_{m0}^2(\beta = \theta, \gamma = \varphi) \left(\sum_{n=-2}^2 D_{0n}^2(g^{-1}) \eta_{mn} \right). \quad (\text{A4})$$

Finally, one finds Eqs. (6) and (8) by replacing g in Eq. (A4) by the two internal three fold rotations around the direction $X+Y+Z$.

-
- [1] T. Niori, T. Sekine, J. Watanabe, T. Furukawa, and H. Takezoe, *J. Mater. Chem.* **6**, 1231 (1996); G. Pelzl, S. Diele, and W. Weissflog, *Liq. Cryst.* **28**, 969 (2001).
- [2] G. Pelzl, S. Diele, and W. Weissflog, *Adv. Mater. (Weinheim, Ger.)* **11**, 707 (1999).
- [3] J. Matraszek, J. Mieczkowski, J. Szydłowska, and E. Gorecka, *Liq. Cryst.* **27**, 429 (2000); E. Matyus and K. Keseru, *J. Mol. Struct.* **543**, 89 (2001).
- [4] Y. Lansac, P. K. Maiti, N. A. Clark, and M. A. Glaser, *Phys. Rev. E* **67**, 011703 (2003).
- [5] R. Pratibha, N. V. Madhusudana, and B. K. Sadishava, *Science* **288**, 2185 (2000).
- [6] L. A. Madsen, T. J. Dingemans, M. Nakata, and E. T. Samulski, *Phys. Rev. Lett.* **92**, 145505 (2004); B. R. Acharya, A. Primak, and S. Kumar, *ibid.* **92**, 145506 (2004).
- [7] M. J. Freiser, *Phys. Rev. Lett.* **24**, 1041 (1970).
- [8] P. G. deGennes and J. Prost, *The Physics of Liquid Crystals* (Oxford University Press, Oxford, 1993).
- [9] W. Maier and A. Saupe, *Z. Naturforsch. A* **13**, 564 (1958); **14**, 882 (1959).
- [10] B. Mettout, P. Tolédano, and V. Lorman, *Phys. Rev. Lett.* **77**, 2284 (1996).
- [11] B. Mettout, P. Tolédano, H. Takezoe, and J. Watanabe, *Phys. Rev. E* **66**, 031701 (2002).
- [12] J. P. Straley, *Phys. Rev. A* **10**, 1881 (1974).
- [13] T. C. Lubensky and L. Radzihovsky, *Phys. Rev. E* **66**, 031704 (2002).
- [14] Yu. M. Gufan, *Structural Phase Transitions* (Nauka, Moscow, 1982).
- [15] S. Jen, N. A. Clark, and P. S. Pershan, *J. Chem. Phys.* **66**, 4635 (1977).
- [16] L. Landau and E. Lifshitz, *Quantum Mechanics* (MIR, Moscow, 1973), Sec. 58.
- [17] A. A. Bul'bich, *Sov. Phys. Crystallogr.* **33**, 629 (1988). The groups C_{2h} and C_i are predicted in this paper as intersections of the usual biaxial nematic symmetry with that of the rectangular laboratory frame. This procedure is implicitly equivalent to taking into account two second-rank tensors.
- [18] G. Nounesis, S. Kumar, S. Pfeiffer, R. Shashidhar, and C. W. Garland, *Phys. Rev. Lett.* **73**, 565 (1994).
- [19] P. J. Collings, D. J. Photinos, P. J. Bos, P. Ukleja, and J. W. Doane, *Phys. Rev. Lett.* **42**, 996 (1978).
- [20] G. Goldfarb, R. Poupko, Z. Luz, and H. Zimmermann, *J. Chem. Phys.* **79**, 4035 (1983); D. W. Allender and J. W. Doane, *Phys. Rev. A* **17**, 1177 (1978).
- [21] T. J. Dingemans, N. Sanjeeva Murthy, and E. T. Samulski, *J. Phys. Chem. B* **105**, 8845 (2001).
- [22] J. Matraszek, J. Mieczkowski, J. Szydłowska, and E. Gorecka, *Liq. Cryst.* **27**, 429 (2000).
- [23] I. Wirth, S. Diele, A. Eremin, G. Pelzl, S. Grande, I. Kovel'enko, N. Pacenko, and W. Weissflog, *J. Mater. Chem.* **11**, 1642 (2001).
- [24] W. Weissflog, H. Nädasi, U. Dunemann, G. Pelzl, S. Diele, A. Eremin, and H. Kresse, *J. Mater. Chem.* **11**, 2748 (2001).

- [25] S. Stojadinovic, A. Adorjan, S. Sprunt, H. Sawade, and A. Jakli, *Phys. Rev. E* **66**, 060701(R) (2002).
- [26] J. A. Olivares, S. Stojadinovic, T. Dingemans, S. Sprunt, and A. Jakli, *Phys. Rev. E* **68**, 041704 (2003).
- [27] P. I. C. Teixeira, A. J. Masters, and B. M. Mulder, *Mol. Cryst. Liq. Cryst. Sci. Technol., Sect. A* **323**, 167 (1998); G. R. Lukhurst, *Thin Solid Films* **393**, 40 (2000); R. Berardi and C. Zannoni, *J. Chem. Phys.* **113**, 5971 (2000).
- [28] T. Dingemans and E. T. Samulski, *Liq. Cryst.* **27**, 131 (2000); C. Chiccoli, I. Feruli, O. D. Lavrentovich, P. Pasini, S. V. Shiyankovskii, and C. Zannoni, *Phys. Rev. E* **66**, 030701 (R) (2002).
- [29] B. R. Acharya, A. Primak, and S. Kumar, *Phys. Rev. Lett.* **92**, 145506 (2004).
- [30] K. Merkel, A. Kocot, J. K. Vij, R. Korlacki, G. H. Mehl, and T. Meyer, *Phys. Rev. Lett.* **93**, 237801 (2004).
- [31] J. Charvolin, *Nuovo Cimento Soc. Ital. Fis., D*, **3**, 3 (1984).
- [32] P. Tolédano, A. M. Figueiredo Neto, V. Lorman, B. Mettout, and V. Dmitriev, *Phys. Rev. E* **52**, 5040 (1995).
- [33] E. A. Oliveira, L. Liebert, and A. M. Figueiredo Neto, *Liq. Cryst.* **5**, 1669 (1989).
- [34] A. Chrzanowska, *Phys. Rev. E* **58**, 3229 (1997).